Study of the interannual ozone loss and the permeability of the Antarctic polar vortex from aerosol and ozone lidar measurements in Dumont dUrville (66.4°S 140°E)

Sophie Godin, Valérie Bergeret, Slimane Bekki, Christine David, Gérard Mégie

JOURNAL OF GEOPHYSICAL RESEARCH, VOL. 106, NO. D1, PAGES 1311–1330, JANUARY 16, 2001

Study of the interannual ozone loss and the permeability of the Antarctic polar vortex from aerosol and ozone lidar measurements in Dumont d'Urville (66.4°S, 140°E)

Sophie Godin, Valérie Bergeret, Slimane Bekki, Christine David, and Gérard Mégie

Service d'Aéronomie du CNRS, Université Pierre et Marie Curie, Paris, France

Abstract. Systematic ground-based measurements of the ozone and aerosol stratospheric profile performed in the Dumont d'Urville (66.4°S, 140°E) Antarctic station are used to study the air subsidence in fall, the springtime ozone loss, and the vortex confinement on an interannual basis. The data obtained mostly from March to October in the 1992 - 1998 time period are analyzed as a function of equivalent latitude in order to discriminate the measurements performed inside, at the edge or outside the vortex. The subsidence rate derived from the ozone measurements in the lower stratosphere prior to the destruction period and from the volcanic aerosol measurements in 1992 is in good agreement with the estimation provided by radiative transfer models. The analysis of the ozone seasonal variation shows that the ozone destruction starts in the beginning of August and affects essentially the inner vortex or inner edge regions. The destruction lasts up to the end of September and low ozone values are found up to the end of October, confirming the isolation of the polar vortex above 400 K. Ozone destruction rates of the order of 3%/d in the 400 - 475 K region and 1.5%/d around 550 K are derived from the data obtained inside the vortex. The ozone measurements obtained in October allow to study the vortex confinement which shows the increase of the ozone meridional gradient through the vortex edge from 400 to 650 K. A fine view of the vortex edge is provided by a near daily series of aerosol lidar measurements performed in October 1992, a period when the vortex was deformed by planetary waves and slanted with respect to the vertical direction.

1. Introduction

Since 15 years, the Antarctic stratospheric ozone hole issue has aroused numerous investigations for the understanding of the evolution of the stratosphere: the depletion of polar ozone in the winter-spring seasons is still an important scientific question for both hemispheres with the annual formation of the ozone hole over increasingly larger areas in Antarctica [*Uchino et al.*, 1999] and increased losses observed in the Northern Hemisphere in the recent years, depending on the meteorology of the Arctic polar vortex [*Rex et al.*, 1997; *Schultz et al.*, 2000]. The various campaigns performed in Antarctica since 1987 provided a clearer understanding of the ozone destruction processes occurring inside the vortex: chemical destruction, driven by reactions involving chlorine and bromine compounds is undoubtedly the cause. However, comparisons with theoretical models show that model simulations tend to underestimate the ozone destruction inside the polar vortex especially in the Northern Hemisphere, which was the subject of extensive studies in the recent years [*Chipperfield et al.*, 1996; *Deniel et al.*, 1998]. Besides, a quantitative explanation of the processes causing mid-latitude trends is still under question: apart from the impact of the Antarctic ozone loss on midlatitude through vortex erosion events and dilution after the final break up, the trends can be linked to heterogeneous chemical reactions on particulate matter such as sulfate aerosols outside the polar vortex as well as to changes in the basic stratospheric dynamics connected somehow to the ozone destruction in the polar vortex. Furthermore, the exchange processes between the polar and midlatitude regions are still not fully quantified and, as stated in the last assessment on stratospheric ozone [*World Meteorological Organization (WMO)*, 1999]: "Until the transport of perturbed air in this region is better understood, it will be difficult to obtain a quantitative understanding of midlatitude ozone depletion" (see also *Solomon*

Paper number 2000JD900459.
0148-0227/01/2000JD900459$09.00

[1999] for a review of the stratospheric ozone depletion issue). Thus, in order to understand the interaction between the polar and midlatitude regions, the interest has focused recently on the area located at the boundary of the polar vortex. In the Southern Hemisphere, this area can affect the populated regions located between 50°and 60°latitude South owing to the increase of the size of the ozone depleted region and the movement of the vortex linked to planetary waves.

The purpose of this article is to analyze a series of ground-based measurements performed in the French base of Dumont d'Urville (66.4°S, 140°E), located on the coast of the Antarctic continent. Continuous ground-based observation of the polar stratosphere is performed since 1988 in this station by the Institut Français de Recherche et de Technologie Polaires (IFRTP), under the scientific responsibility of the Service d'Aéronomie du CNRS (SA-CNRS). This program includes measurements of the ozone and NO_2 total contents by a SAOZ (Système d'Analyse par Observation du Zénith) UV-Visible spectrometer [*Pommereau and Goutail,* 1988] and of the stratospheric vertical profile of ozone and aerosols by ozone sondes and lidar [*Godin et al.,* 1994a]. The electrochemical concentration cell (ECC) ozone soundings are performed since 1990 with an increased rate during the ozone destruction period in winter and early spring. The lidar measurements are performed in the frame of the Polar Ozone Lidar Experiment (POLE) project in cooperation with the CNR-IROE of Florence since 1989 for the aerosol and polar stratospheric clouds and since 1991 for the ozone vertical distribution. In parallel, radiosondes are launched daily by the French Meteorological Office for the measurement of local pressure and temperature vertical profiles. These measurements were compared to UARS satellite measurements in a recent study on the temporal evolution of stratospheric constituents above Dumont d'Urville, from August 14 to September 20, 1992 [*Ricaud et al.,* 1998]. In this work, the time evolution of the measurements were interpreted by comparison with results from a three-dimensional chemical transport model. A general agreement was found between the measured data sets throughout the stratosphere. The agreement between the model and the measurements was better in the middle than in the lower stratosphere. In particular, the model underestimated the ozone destruction at 46 hPa.

In winter, the dominant processes affecting the Antarctic stratosphere after the formation of the polar vortex are the air subsidence due to infrared cooling and the formation of polar stratospheric clouds when the temperature drops below a certain threshold (195 K around 18 km). In spring, the ozone seasonal variation inside the vortex is controlled by the chemical destruction due to the activation of chlorine and bromine compounds on particulate matter [*WMO,* 1999]. The climatology of the various types of polar stratospheric clouds (PSC) observed at Dumont d'Urville was analyzed in detail in a previous publication [*David et al.,* 1998], so our objective here is to use the long-term time series of ozone and aerosol vertical distribution obtained at this station to study the air subsidence and the ozone loss on an interannual basis. The evaluation of the subsidence from the stratospheric aerosol measurements is limited to the period of observation of the volcanic aerosols injected in the stratosphere by the eruption of Mount Pinatubo in 1991. Besides, the Dumont d'Urville station, located at a latitude of 66.4°S at the shore of the Antarctic continent, is particularly well suited to study polar processes at the edge of the vortex: the measurements can sample air alternatively inside or outside the polar vortex as the vortex moves above the continent. This particular position allows to study the permeability of the polar vortex as a function of altitude. It induces also an additional day-to-day variability which necessitates the classification of the data with respect to the position of the polar vortex.

This paper is organized as follows: after a description of the main characteristics of the aerosol and ozone measurements, the temporal evolution of the position of Dumont d'Urville with respect to the polar vortex is discussed. The seasonal evolution of the ozone mixing ratio as a function of altitude inside, at the edge and outside the polar vortex is then analyzed. The three following sections are devoted to (1) the evaluation of the air subsidence in 1992 using the aerosol lidar measurements obtained a year after the Pinatubo eruption in 1991 and the ozone measurements in autumn prior to the ozone depletion period, (2) the determination of the ozone destruction rates from 1993 to 1998 at various isentropic levels and (3) the study of the vortex edge from 400 to 650 K using the measurements performed alternatively inside and outside the vortex in spring.

2. Description of the Measurements

The multiwavelength lidar instrument was described in detail by *Stefanutti et al.* [1992]. At the present time, it is the only mixed ozone/backscatter lidar operating routinely on the Antarctic continent. The lidar transmitter includes two laser sources, a XeCl exciplex laser and a Nd:Yag laser which provide the wavelengths necessary for both the aerosol and the ozone measurements. The operation of the lidar requires nighttime and quasi clear sky conditions so no lidar measurements are obtained in the summertime owing to the very short nights and year round in bad meteorological conditions. The ozone and aerosol lidar measurement are performed each day sequentially when the experiment is possible, following a protocol based on the period of interest: an intensive aerosol period from May to July in order to study the formation of the Polar Stratospheric Clouds (PSCs), followed by an intensive ozone period from August to November to study the ozone destruction.

2.1. Aerosol Measurements

The second harmonic (532 nm) of the Nd:Yag laser is used for the particles observation [*Stefanutti et al.*, 1991; *David et al.*, 1998]. The parallel and perpendicular components of the 532 nm radiation are detected simultaneously in order to retrieve the backscatter and depolarization ratios of the aerosols or PSCs. In the present study, we use only the volcanic aerosol measurements obtained after the eruption of Mount Pinatubo in 1991. Consequently, only the backscatter ratio is considered since the background or volcanic aerosol are mainly liquid particles which hardly depolarize the laser light. The backscatter ratio is defined as the ratio of the total backscatter coefficient (the sum of the molecular and aerosol backscatter coefficient) to the molecular backscatter coefficient.This parameter is retrieved using the Klett method, with a fix backscatter to extinction ratio of 0.025. The molecular backscatter coefficient is computed from the pressure and temperature (PTU) measurements obtained daily at the station. The accuracy of the measurement is of the order of 5% - 8% with a vertical resolution of 0.1 km and a temporal resolution of 30 min. The injection of massive amounts of sulphur following the eruption of Mount Pinatubo in 1991 provided the opportunity to study the permeability of the polar vortex as the volcanic cloud reached the polar regions in the spring of 1991. The cataclysmal eruption of Mount Pinatubo (15°N, 120°E), considered as one of the major eruption of the century for the climatic impact, took place in June 1991. High amounts of ash, dust, and sulfur dioxide were injected directly into the stratosphere, up to at least 30 km. The total mass of SO_2 was estimated to 12 - 15 Mt from the spectral measurements of the Solar Backscatter Ultraviolet instrument (SBUV/2) [*McPeters*, 1993]. The sulfur dioxide injected into the stratosphere was rapidly converted photochemically to sulfuric acid vapor (H_2SO_4) which formed through nucleation and condensation processes, liquid droplets of sulfuric acid solution [*Hamill et al.*, 1996]. The exponential decay time of the peak backscatter ratio was estimated to 1 ± 0.2 years (see chapter 3 of [*WMO*, 1999] for a summary of the characteristics of the Mount Pinatubo volcanic cloud).

As indicated by a previous publication [*Godin et al.*, 1996], the Pinatubo aerosols were detected unambiguously from the beginning of September 1991 in Dumont d'Urville. Our measurements did not show any intrusion of the Pinatubo volcanic aerosol inside the vortex prior to mid-October 1991, in contrast with the small cloud originated from the eruption of Mount Cerro Hudson in August 1991 and located in the very low stratosphere around 12 km. This cloud could be detected on each measurement whatever the position of the station with respect to the vortex, while the Pinatubo cloud located above 20 km during this period was detected exclusively outside the vortex. From January to November 1992, 131 aerosol lidar measurements were obtained, allowing thus to study in detail the parallel evolution of the volcanic cloud inside or outside the vortex. For the winter season of 1992, care was taken to avoid the measurements contaminated with PSCs, according to the method developed by *David et al.* [1998]. This implies that less measurements are taken into account especially in July and August 1992.

2.2. Ozone Measurements

The vertical distribution of ozone is measured by lidar in the stratosphere from 12 to 40 km, using the differential absorption method [*Godin et al.*, 1992]. The absorbed wavelength (308 nm) is provided by the exciplex laser and the reference wavelength (355 nm) corresponds to the third harmonic of the Nd:Yag laser radiation. The ozone number density is computed from the difference of the slopes of the signals originated from the Rayleigh scattering of the emitted laser beam. Since the lidar signals cover a very high dynamical range, the Rayleigh signals have to be attenuated for the measurements in the low stratosphere. The final ozone measurement corresponds thus to a composite profile computed from the "high" and the "low" Rayleigh signals which are detected simultaneously since 1996 (previously, both measurements were obtained sequentially). A typical experiment lasts 3 - 4 hours, leading to a horizontal spatial resolution of 100 - 200 km. The vertical resolution ranges from 0.5 km at 12 km to 4 km at 35 km, with a corresponding total uncertainty varying from 3 to 15% in the same altitude range and in the absence of PSCs. Indeed, a correct retrieval of the ozone number density is impossible in the presence of PSCs or volcanic aerosol at the altitude of the cloud. In this case, ozone profiles are provided above the altitude of the cloud. Thus the ozone lidar measurements performed in 1992 are not discussed here because of the contamination of the data by the Mount Pinatubo volcanic aerosol in the lower stratosphere. In the beginning of 1993 and 1994, the aerosol layer was down to 16 km (420 K) and 12 km (350 K), respectively. An aerosol correction on the ozone data was performed, using assumed values of the aerosol angström coefficients for the backscatter and extinction terms in the ozone lidar equation [*Godin et al.*, 1994b]. These assumptions were derived from the measurements of the size distribution of the Mount Pinatubo volcanic aerosols performed by *Deshler et al.* [1993]. This correction is, however, not efficient in the case of high volcanic aerosol amounts or strong PSC events. Although the volcanic aerosol amount had decreased in 1993, the ozone measurements around 400 K have thus to be considered with caution, for at least the first 6 months. From 1996, the amount of aerosol is close to the background level in the whole stratosphere, so no aerosol correction is performed. Besides, for the whole time period considered here, the ozone measurements contaminated by the presence of PSCs are suppressed from the database. Finally, no ozone lidar measure-

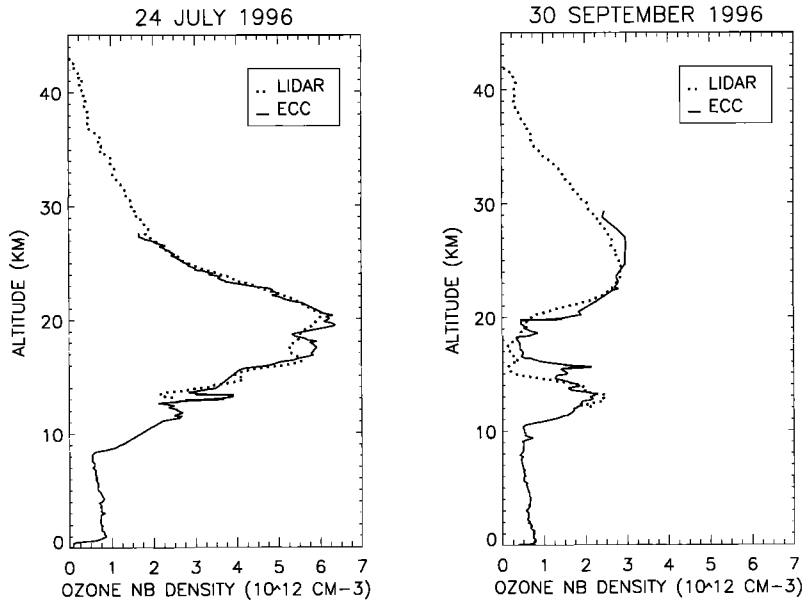

Figure 1. Comparison of ozone profiles obtained on the same day with ECC sondes and the ozone lidar, prior and during the ozone hole period in 1996.

ments were obtained in 1995 owing to a failure of the exciplex laser, so this year will not be considered in this study.

The ECC sondes provide ozone profiles from the ground to 25 km in average. They are coupled to Vaïsala sondes measuring the humidity, pressure, and temperature. Their accuracy is of the order of 8% with a vertical resolution of $\sim$ 0.2 km. A good agreement is generally observed between the lidar and the ECC sondes, when the measurements are performed in the same airmass (see Figure 1 which shows ozone profiles obtained before and during the depletion period in 1996), so these measurements are considered to be complementary, the ECC sondes allowing to obtain ozone measurements when the lidar cannot be operated (bad weather, summer period). The improvement of the launching procedure allowed to increase the maximum altitude reached by the balloon especially in winter. From 20 km in the winter of 1990, the balloons reach now routinely an altitude of 28 km even in the lowest temperatures. The number of measurements obtained by each instrument is summarized in Table 1, for the various years considered in this study.

3. Position of Dumont d'Urville With Respect to the Antarctic Polar Vortex

The Dumont d'Urville station is located at (66.4°S, 140°E), on the coast of the Antarctic continent. As mentioned previously, this position induces an additional day-to-day variability from fall to spring due to the alternate sampling of the air inside or outside the polar vortex as the vortex wobbles above the continent. For instance, strong daily variations reaching 100 DU in October are currently observed in the total ozone measurements, in correlation with the passage of the vortex above the station. Similar variations are observed also on the ozone lidar and sondes profiles. In order to analyze properly the temporal evolution of the ozone and aerosol content, the data have to be classified according to the position of the station with respect to the polar vortex. The method employed here is the following: the equivalent latitude of the station at various potential temperature levels is determined, and the data are remapped in this potential temperature - equivalent latitude coordinate system. The equivalent latitude is a modified potential vorticity (PV) variable defined as the latitude enclosing the same area as the PV contour. The conservation of PV or equivalent latitude and potential temperature in the middle atmosphere under adiabtic frictionless motions allows us to use these variables as alternate coodinates [*McIntyre and Palmer,* 1984; *Butchart and Remsberg,* 1986]. The meteorological fields are obtained from the United Kingdom Meteorological Office (UKMO) with a temporal resolution of 24 hours and a spatial resolution of 2.5° in latitude and 3.75° in longitude. The vertical resolution is close to 2.5 km in the lower stratosphere, the region of interest here. The potential temperature levels

Table 1. Number of Ozone Lidar and Sondes Measurements in the 1993-1998 Period

Year	1993	1994	1996	1997	1998
Lidar	30	44	68	63	35
Sondes	30	29	23	23	24

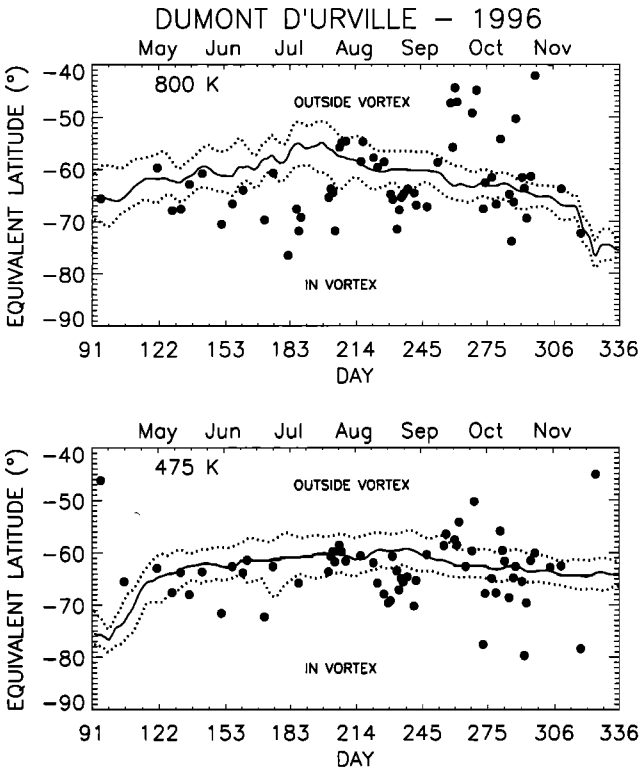

Figure 2. Evolution of the position of Dumont d'Urville in equivalent latitude during the winter and spring of 1996 at 475 and 800 K (black dots). The solid line corresponds to the limit of the vortex while the dashed lines indicate the boundaries of the vortex edge.

used in this study range from 400 to 650 K. The method used to determine the position of the polar vortex follows the approach of *Nash et al.* [1996], which uses the maximum gradient of PV as a function of equivalent latitude: the vortex limit corresponds to the maximum gradient of potential vorticity as a function of equivalent latitude constrained by the location of maximum wind jet, while the inner and outer boundaries of the vortex edge are defined from the local extrema of the second derivative of the potential vorticity. The results of this classification are represented in Figure 2 which shows the temporal evolution of the position of Dumont d'Urville in equivalent latitude together with the position of the vortex, from April 1 to November 30, 1996, at 475 and 800 K potential temperature levels. The time series corresponding to the vortex limit and both vortex borders are smoothed using a running average of 7 days in order to reduce the noise inherent to the computation method. The dots showing the position of the station in equivalent latitude correspond to the dates of the ozone lidar and ECC measurements in 1996. Figure 2 shows that the vortex starts to form in the middle stratosphere and propagates down to lower levels in autumn, in agreement with *Manney and Zureck,* [1993]. In consequence, the classification method is less efficient during this season, owing to the flatness of the PV fields, especially in the lower levels. The levels located under 400 K for instance are difficult to classify before July. Figure 2 shows the variability of the position of Dumont d'Urville relative to the polar vortex, as a function of the isentropic level and the season: in autumn of 1996, the measurements are performed mostly inside and in the inner edge of the vortex at both levels. In winter, the vortex area is larger in the middle stratosphere than in the lower stratosphere: at 800 K the outer edge of the vortex reaches 52° equivalent latitude as compared to 57° at 475 K. The measurements performed in August are more deeply inside the vortex at 800 K than at 475 K. The decrease of the vortex area begins earlier in the middle stratosphere than at lower levels: at 800 K the decrease of the vortex area is observed from the beginning of August with a marked decrease in November. At 475 K the vortex area shows a small decrease from September, but the vortex stays relatively stable up to the end of November. Besides, the spring season is characterized by a higher variability at both levels with alternate situations inside and outside the vortex. In the middle stratosphere the vortex is deformed by planetary waves which explains the low absolute values of the station equivalent latitude, reaching 45° in mid-September. The analysis of the position of the station as a function of altitude reveals a large interannual variability, as shown in Figure 3, which represents the proportion of "inside," at the "edge" or "outside" vortex situations as a function of the potential temperature and the season in 1993, 1994, and 1996. Only these years are discussed here, since they are representative of the interannual variability of the Dumont d'Urville equivalent latitude over the whole 1992-1998 period. In Figure 2, the percentages are relative to the whole classification period and not to the total number of observations, but the statistics of the measurements, which are sometimes performed every other day in winter and spring, follow these general characteristics. Figure 2 confirms that the equivalent latitude of Dumont d'Urville varies with altitude, which implies that care has to be taken in the analysis of the vertical profile data. In autumn, the station is mostly located at the edge of the vortex, in the whole altitude range in 1993. The number of "inside" situations increases with altitude while the number of "outside" situations decreases except at the lower most levels 400 and 430 K for which the results are more doubtful due to the less efficiency of the classification method. This behavior is consistent with the vortex formation in the higher levels in autumn. In 1996, the position of Dumont d'Urville shows the same behavior except around 475 K where more "outside" than "inside" situations are observed. In contrast in 1994, the station is at 70% outside the vortex and never inside. In winter, when the vortex area is largest, the station is mostly inside the vortex. In 1993, the station is inside the vortex for more than 60% of the time and in the edge region for the remain-

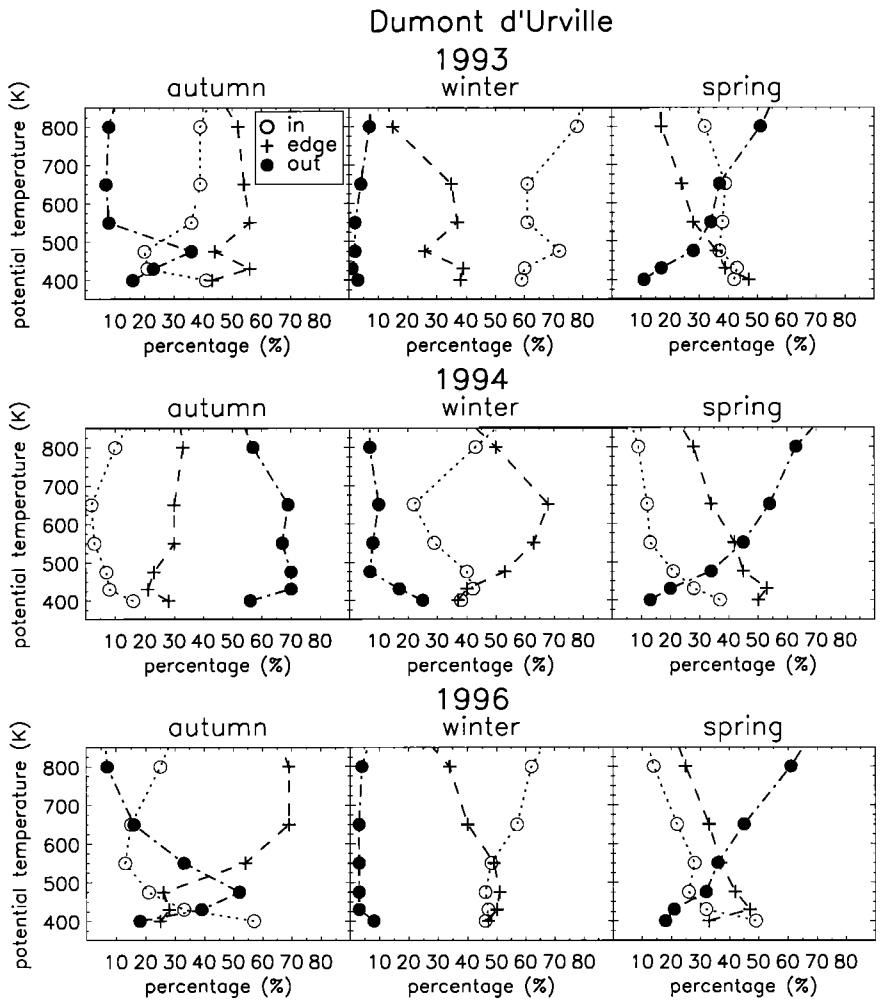

Figure 3. Sampling frequency of the three regions: "in," "edge," and "outside" the vortex in 1993, 1994, and 1996 as a function of the potential temperature and the season.

ing 40% especially at low altitude levels. In 1996, the "inside" and "edge" situations are equally observed in the lower stratosphere, while "inside" vortex situations are dominant in the middle stratosphere. The number of "outside" situations is negligible. In 1994, the station is mostly in the edge of the vortex in the middle stratosphere and equally inside and in the edge in the lower stratosphere. The number of "outside" situations, reaching 30% at 400 K is, however, higher than in the other years at these levels. In spring, the number of "outside" situations increases with altitude and becomes generally dominant above 600 K. This feature is most pronounced in 1994 and in 1996. This is consistent with the earlier decrease of the vortex area and the less stability of the vortex due to the action of the planetary waves at higher altitude. In the middle stratosphere, more "inside" than "edge" cases are observed in 1993, the situation being reversed in 1994 and 1996. In the lower stratosphere the "inside" and "edge" situations are equally observed in 1993, while in 1994 and 1996, the station is mostly in the vortex edge. These results prefigure already our ability to study the evolution of the ozone or aerosol amounts in the various regions. For instance, the good sampling of the inner vortex region in 1993 allows a better evaluation of the ozone destruction rates than in 1994, a year when Dumont d'Urville proved to be the most outside the vortex over the whole 1992-1998 period. The year 1996, as well as the other years not discussed here, represent somewhat intermediate situations between these two extremes.

4. Seasonal Variation of the Ozone Mixing Ratio as a Function of Altitude Inside, at the Edge and Outside the Polar Vortex

The ozone measurements in Dumont d'Urville show that the shape of the ozone mixing ratio vertical profile varies substantially as a function of the season and the position of the station with respect to the polar vortex. This is illustrated in Figure 4 which shows examples of ozone lidar profiles obtained inside, at the edge and outside the polar vortex in May, August, and October 1997. In autumn under about 500 K, the ozone mixing

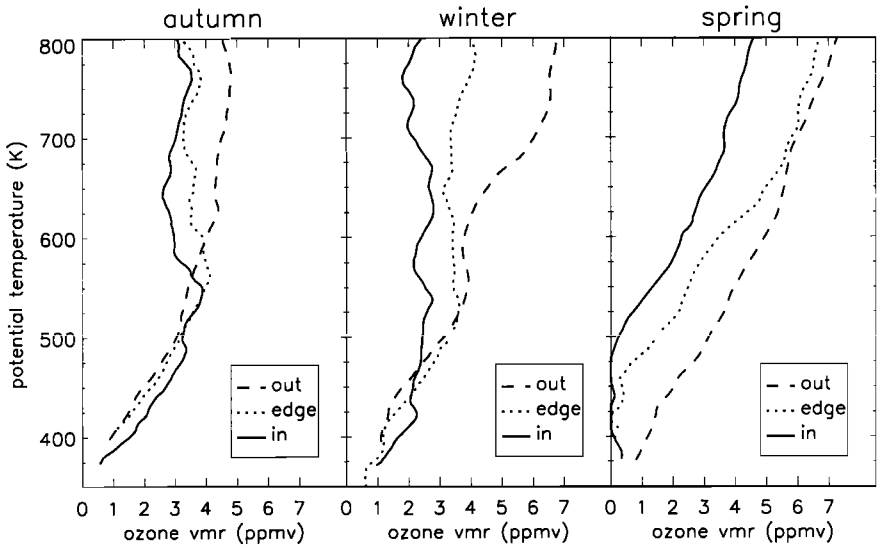

Figure 4. Examples of ozone lidar profiles obtained inside, in the edge region and outside of the vortex in autumn, winter, and spring.

ratio shows a positive gradient as a function of increasing equivalent latitude and a strong positive gradient as a function of increasing potential temperature. Above this level, the situation is reverse: the vertical gradient of ozone is weak, and the ozone mixing ratio decreases as a function of increasing equivalent latitude. In winter, a similar global pattern is observed with alike vertical and horizontal gradients. The ozone profile inside the vortex was obtained in the beginning of August, prior to the beginning of the ozone destruction, so the ozone amount is still high in the lower stratosphere. In spring, the vertical gradient of ozone becomes positive both inside and in the edge region in the middle stratosphere while the ozone gradient as a function of increasing equivalent latitude is still negative. In the lower stratosphere, the horizontal ozone gradient is now also negative due to the ozone destruction which takes place both inside the vortex and in the edge region. For the measurements performed inside the vortex, the ozone destruction is complete from 400 to 500 K.

In order to give a more systematic view of the ozone seasonal variation above Dumont d'Urville, the temporal evolution of the ozone mixing ratio retrieved from the measurements performed in 1993, 1994, 1996, 1997, and 1998 is represented in Figure 5 from 400 to 650 K. The data are classified according to the position of the polar vortex with respect to the station and no distinction is made between the ECC sondes and the lidar measurements, owing to the good agreement found between both techniques when similar air is sampled. The dashed lines mark the limit of the classification period from April 1 to November 30. The square symbols represent the data obtained before and after this period. During the classification period, measurements performed inside and outside the vortex are represented by open circles and filled circles, respectively. The edge region is further divided in two regions: the inner edge located between the inner vortex border and the vortex limit, and the outer edge located on the opposite side of the vortex limit. The measurements performed in the inner and the outer edges are represented by pluses and crosses, respectively. It has to be kept in mind that the data classification is more uncertain in April and around 400 K up to July. Furthermore, throughout the year, the classification is affected by the noise inherent to the method: despite the smoothing applied to the data, the error on the position of the inner and outer vortex borders is evaluated to about 2° equivalent latitude, so data categorized inside the vortex for instance can in reality belong to the inner edge region. This has for effect to blur the picture for the measurements performed when the equivalent latitude of the station is close to one of the vortex borders. In spite of this effect, the classification of the measurements shows the main features of the dynamical and chemical behavior of the air masses inside and outside the vortex. The dominant processes affecting the ozone seasonal variation inside the vortex in the lower stratosphere are the air subsidence due to infrared cooling in autumn and winter and the chemical destruction in winter and spring. In parallel, horizontal mixing within the inner vortex area characterized by rather weak PV gradients tends to flatten the ozone latitudinal gradients. Outside the vortex, the ozone content is controlled in winter and spring by downward and poleward transport which brings high ozone amounts from the low-latitude regions where ozone is formed. Total ozone measurements performed in the Southern Hemisphere showed that the ozone spring maximum is most pronounced outside the vortex due to the presence of a strong polar vortex, in contrast with the Northern Hemisphere where the peak total ozone abundance is observed around 75°N [*London*, 1985].

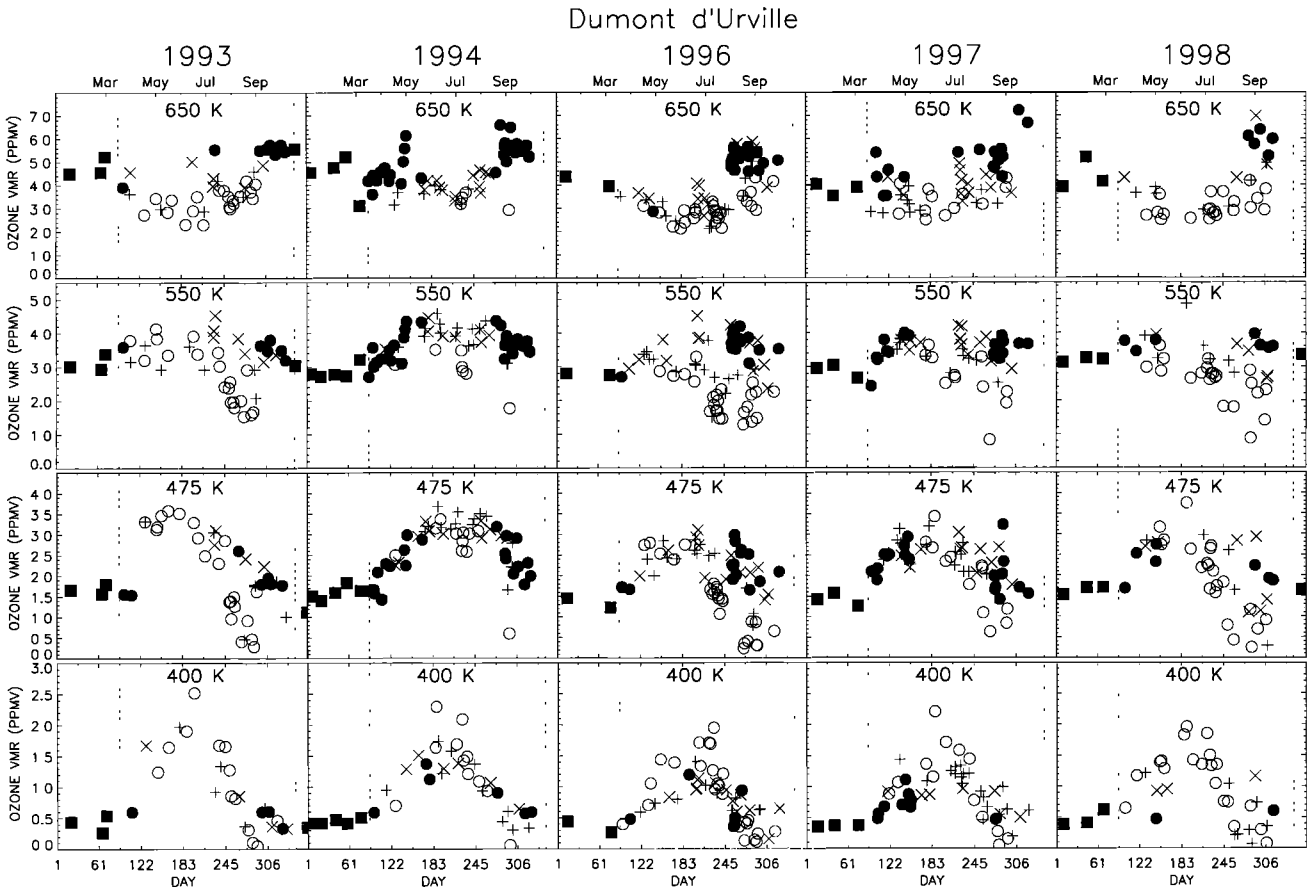

Figure 5. Temporal evolution of the ozone mixing ratio sorted with respect to the position of the polar vortex in 1993, 1994, 1996 and 1998. The dash lines mark the classification period, from April 1 to November 30. Data obtained in summer are represented by filled squares. Within the classification period, measurements obtained inside, in the inner edge, in the outer edge, and outside the vortex are represented by open circles, pluses, crosses, and filled circles respectively

The effect of the subsidence on the ozone amount is strongest in the lower stratosphere where the ozone vertical gradient is highest. Above the ozone maximum, the vertical gradient is weak especially inside the vortex, and the effect of the subsidence should be small. The ozone increase in the lower stratosphere due to the subsidence at one particular level stops when the ozone maximum is reached. As seen in Figure 5, the ozone maximum is reached in August at 400 K, in June at 475 K, and in May at 550 K. The large range of ozone values observed in the winter of 1996 at 550 K is due to this differential effect: lower ozone amounts are already observed inside the vortex, while an ozone increase is still observed in the outer edge region.

In autumn, no clear distinction in the evolution of the ozone amount can be made between the various regions, although maximum ozone values at 400 K seem generally to be reached by measurements performed inside the vortex. The sampling of the ozone field by the ground-based measurements in Dumont d'Urville does not allow to differentiate the subsidence inside or outside the vortex. Furthermore, additional effect linked to horizontal mixing have to be considered here.

From August to October, two classes of data can be distinguished according to the evolution of the mixing ratio: inside the vortex and in the inner edge, the rapid decrease of the ozone amounts up to 550 K is due to the ozone destruction caused by the heterogeneous reactions involving active chlorine compounds. At 400 K the distinction between the various regions is weak, and some low values are observed in measurements performed outside the vortex or in the outer edge, in 1996 for instance. However, complete ozone destruction is observed inside the vortex and in the edge region in October. At 475 K the distinction between the ozone destruction inside the vortex and the ozone evolution outside the vortex is clearer. Near complete ozone destruction is generally reached at the end of September. In 1994 measurements performed in mid-August likely show the start of an ozone destruction, but the inner vortex region is poorly sampled afterward. No destruction rate can thus be deduced from the measurements at this level. However, a good sampling of the outside region is achieved in 1994. This allows us to visualize the behavior of ozone in this region in autumn and winter up to 650 K, which is barely the case in the other

years. Besides, the rather low ozone values observed outside the vortex in October 1997 are characterized by an equivalent latitude of 20°S and 30°S, indicating the presence of subtropical air above the station. At 550 K an ozone decrease is observed inside the vortex and in the inner edge in August and September, but it does not reach complete destruction as in the lower levels. In October, the measurements performed inside the vortex present a large variability, particularly in 1996 when a good sampling of the ozone field was achieved. The analysis of the measurements as a function of the equivalent latitude shows that the higher ozone amounts inside the vortex correspond to measurements close to the vortex edge (see section 7). Ozone destruction is also observed in the inner vortex edge at this level, but it seems smaller than the one observed inside the vortex. More generally, a clear distinction can be made between the inner edge and the outer edge ozone values at 475 and 550 K, except in 1994 when the measurements barely sampled the ozone destruction. The inner edge ozone amounts are close to those obtained inside the vortex, while the outer edge values follow those obtained outside the vortex. This illustrates the weak mixing within the edge region.

At 650 K the temporal evolution of the ozone mixing ratio is different: it shows a decrease in fall and an increase in spring, with higher ozone amounts observed outside the vortex and in the outer edge at the latter season than inside the vortex or in the inner edge. The ozone decrease in fall is due to the subsidence and the horizontal mixing consecutive to the formation of the polar vortex. In July and August the ozone mixing ratio remains constant, which is consistent with the weak vertical ozone gradient inside the vortex and the stability of the vortex itself. No clear ozone destruction is detected from the data in the August-September period, but as indicated by *Manney et al.* [1995], the ozone destruction can be masked by dynamical processes, mainly the diabatic descent, still occurring in the middle stratosphere in spring.

Finally, Figure 5 shows, to some extent, the interannual variability of the ozone seasonal variation, despite the different sampling: the maximum ozone amounts reached at 400 K in 1996 and 1998 are lower than in 1993 and 1994. At 475 K, the maximum ozone in 1996 is still low as compared to the other years. Ozone amounts inside the vortex at 550 K in winter are also smaller in that particular year. This variability reflects the variability in the ozone transport in the Southern Hemisphere linked to dynamical processes such as the quasi-biennal oscillation [*Butchart and Austin*, 1996].

In sections 5 and 6 we attempt to quantify the air subsidence and the ozone destruction from the measurements performed in Dumont d'Urville. The quantification is made only inside the vortex, since the large gradients characterizing the vortex edge in both the ozone and aerosol fields, together with the limited temporal sampling, do not allow us to obtain valid results on the processes to be characterized. In these studies, we generally make the assumption that the Antarctic polar vortex is relatively well mixed within the area covered by the measurements during the period under study and that horizontal transport and mixing has a smaller contribution to the evolution of the ozone or aerosol amount than the subsidence and the chemical destruction. Indeed, ground-based measurements provide reliable measurements in the lower stratosphere, but their limited spatial coverage prevents an accurate quantification of meridional gradients necessary to quantify the influence of meridional advection and horizontal mixing. Moreover, the measurements performed inside the vortex generally span an equivalent latitude range less than 10°, limiting thus the error made in neglecting the meridional gradient as a function of equivalent latitude. The mixing properties of the Antarctic polar vortex were the object of numerous investigations which generally show that the Antarctic inner vortex region is relatively well mixed, although less than the midlatitude "surf zone": *Bowman* [1993] computed a diffusion coefficient of the order of 10^5 m^2s^{-1} at 450 K inside the vortex compared to 5 - 10 x 10^5 m^2s^{-1} outside the vortex. In a detailed study of the structure of the polar vortex in the austral spring of 1987, *Schoeberl* [1992] found values between 10^4 m^2s^{-1} in the vortex edge and 10^5 m^2s^{-1} inside the vortex, compared to 5 x 10^5 m^2s^{-1} outside the vortex. In a later study, the quasi-horizontal transport and mixing in the Antarctic stratosphere was investigated with a semi-Lagrangian transport model and a "contour advection" technique in the winter and spring of 1992 by *Chen et al.*, [1994]. Their results suggest that passive tracers are well mixed inside the vortex and in the midlatitude "surf zone." Calculations of the lengthening of material contours using the contour advection technique show that in the lower stratosphere strong stirring occurs in the inner vortex.

5. Evaluation of the Air Subsidence in the Lower Stratosphere

5.1. Aerosol Measurements

In the absence of chemical processes, the air subsidence around Dumont d'Urville can be evaluated from the volcanic aerosol measurements performed in 1992 and from the ozone measurements obtained in the various years during the fall season. This evaluation is made in the low stratosphere, a region where the bulk of the Mount Pinatubo volcanic aerosol cloud is located in 1992 and where the ozone vertical gradient is most pronounced. In the following studies, the subsidence rate is defined as the descent rate through the isentropes and corresponds to $d\theta/dt$.

In 1992 the first signature of the vortex formation on the aerosol measurements was detected on April 17, when a descent of the whole aerosol layer coincided with the appearance of a clear signal on the PV gradient

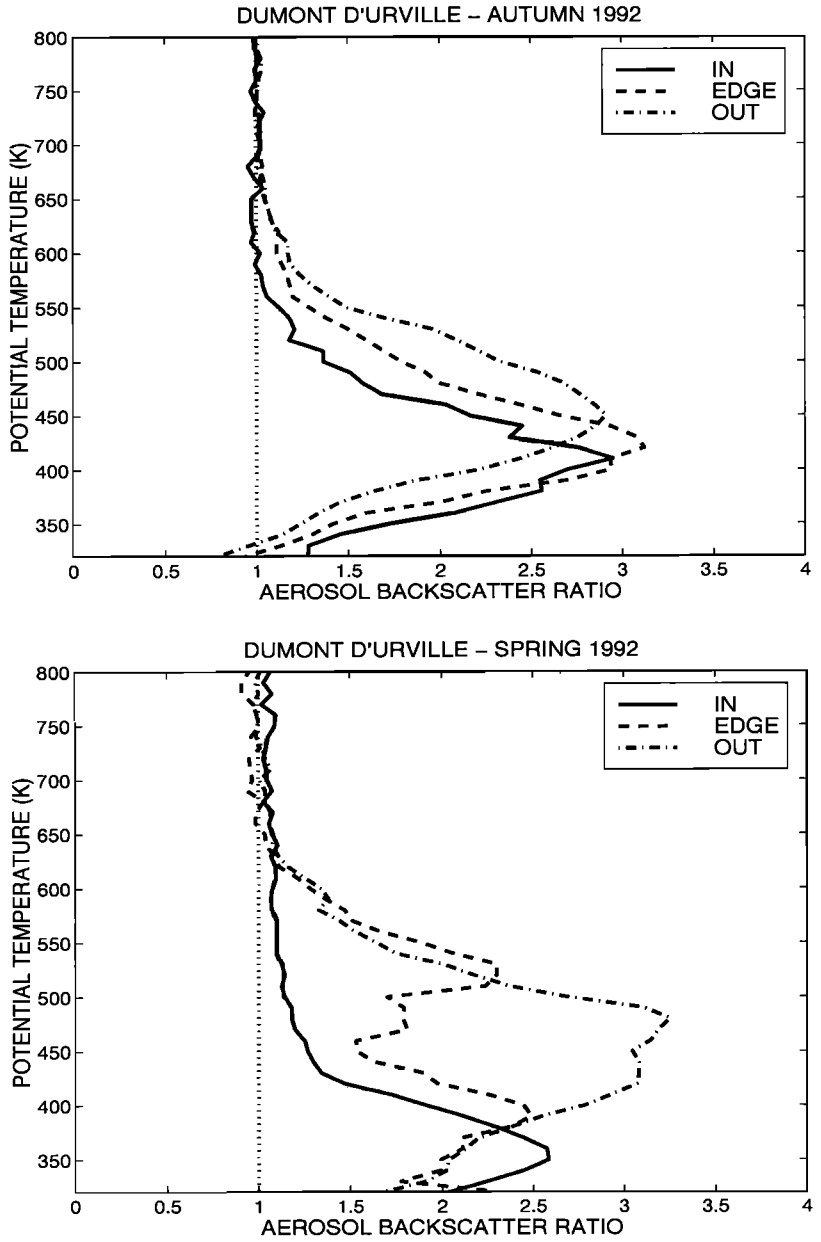

Figure 6. Average lidar profiles of aerosol backscatter ratio obtained inside, in the edge region and outside the vortex in the autumn and spring of 1992

field. The descent of the volcanic aerosol layer in 1992 is illustrated in Figure 6, which shows the seasonal average of the aerosol backscatter ratio in autumn (May-June) and in spring (September-October) inside, in the edge region and outside the polar vortex. The average is calculated as a function of potential temperature in order to reduce the scatter due to adiabatic transport processes in each region. In autumn the three regions show similar values of the average maximum backscatter reaching about 3, but the altitude of the aerosol layer is the lowest inside the vortex, since the maximum backscatter ratio is located slightly above 400 K, as compared to 430 K in the edge region and 450 K outside the vortex. These results illustrate the difference in the dynamical processes around the vortex edge region. The mean equivalent latitude of the measurements averaged outside the vortex is 53°S, at $\sim 9°$ of the outer vortex border, compared to 70°S, at $\sim 8°$ of the internal vortex border for the measurements averaged inside the vortex. In the springtime, the aerosol layer inside the vortex has subsided down to 350 K. In the edge region, the backscatter ratio shows a double peak, with the lower peak located slightly above the maximum backscatter ratio inside the vortex. The double peak structure is due to the fact that the vortex was deformed by planetary waves in October and slanted with respect to the vertical. So during this period, the lidar measurements sampled the regions located inside

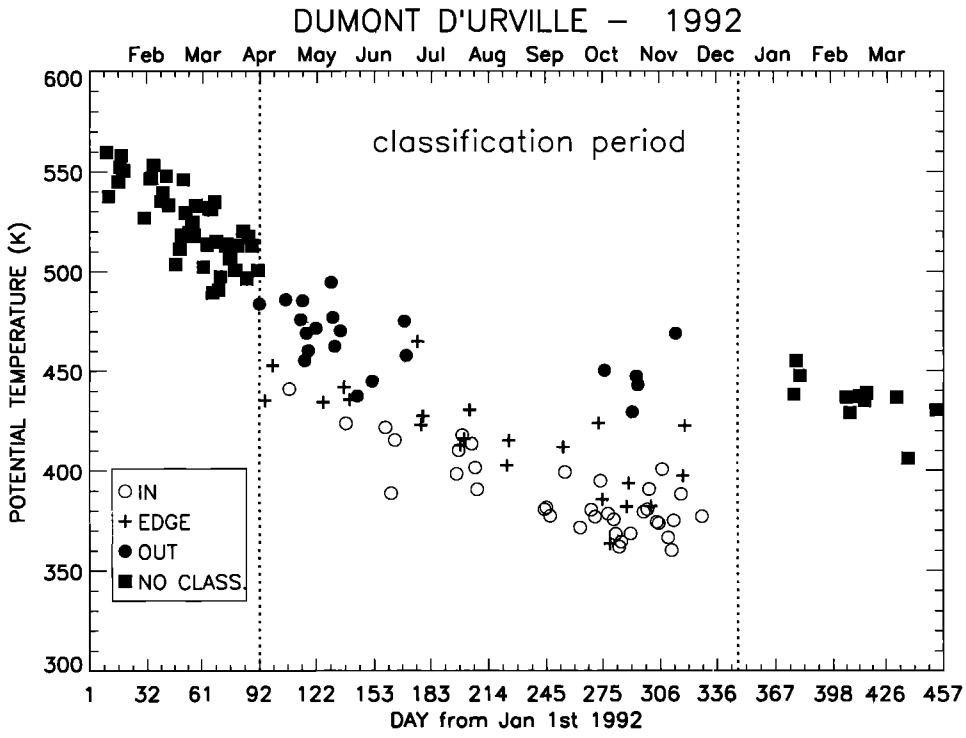

Figure 7. Temporal evolution of the barycentric potential temperature of the volcanic aerosol layer in Dumont d'Urville in 1992 and 1993. The data are classified according to the position of the station with respect to the polar vortex

or the edge of the vortex in the lower stratosphere and the region located outside the vortex above. In these measurements, the maximum backscatter ratio was located in the lower levels, while part of the aerosol cloud located outside the vortex was detected when the laser beam crossed the vortex edge. All the measurements performed during this period are detailed later in the study of the vortex's permeability. Outside the vortex, the aerosol layer presents also a double peak structure but less pronounced than in the edge region. Furthermore, the value of the backscatter ratio around 350 K is higher than in autumn. This could be explained by the higher permeability of the vortex at these low altitudes allowing thus the aerosols which subsided inside the vortex to penetrate in the outside region.

In order to evaluate the diabatic descent from the volcanic aerosol data, we consider the temporal evolution of the barycentric potential temperature of the backscatter ratio vertical distribution. The barycentric potential temperature is preferred to the altitude of the maximum backscatter ratio in order to smooth the influence of localized peaks in the aerosol cloud. It is computed as follows:

$$\Theta_{bar} = \frac{\int_{\theta_1}^{\theta_2} \theta R(\theta)\, d\theta}{\int_{\theta_1}^{\theta_2} R(\theta)\, d\theta}, \qquad (1)$$

where $R(\theta)$ is the backscatter coefficient and θ_1 and θ_2 are the minimum and maximum potential temperature levels of the volcanic aerosol layer, respectively. The temporal evolution of Θ_{bar} is represented in Figure 7. The measurements are classified according to the position of the station with respect to the polar vortex, with similar symbols as in Figure 5, except that no distinction is made between the inner and outer vortex edge. In order to take into account the lowering of the aerosol layer, the classification is made at the barycentric potential temperature of the aerosol layer, which implies that the position of the vortex, determined initially at given levels, is interpolated at Θ_{bar} for each measurement. Figure 7 shows clearly the descent of the volcanic aerosol cloud from the formation of the polar vortex in the beginning of April, with systematically lower barycentric potential temperature values for the measurements performed inside the vortex. According to the measurements, the subsidence around 400 K inside the vortex lasts up to the end of August. After this period, the aerosol layer stays roughly at the same potential temperature level. In the edge region, the aerosol layer is located at higher potential temperature levels, indicating a somewhat lower subsidence. It is impossible to evaluate the rate of diabatic descent in this region taking into account the high aerosol gradient and the inherent variability of the station's equivalent latitude through this area. Inside the vortex, the global descent of the aerosol layer is mainly due to the air diabatic descent and to the sedimentation of the particules. The diabatic descent rate can then be evaluated from the temporal evolution of Θ_{bar} according to the following formula:

$$\frac{d\Theta_{bar}}{dt} = \frac{d\theta_d}{dt} + \frac{d\theta_s}{dt}, \quad (2)$$

where the first term of (2) corresponds to the diabatic descent rate and the second to the descent due to the sedimentation of the particles. The latter term is related to the fall velocity v_s of the particles by:

$$\frac{d\theta_s}{dt} = \frac{\partial\theta}{\partial t} + v_s\frac{\partial\theta}{\partial z}. \quad (3)$$

$d\Theta_{bar}/dt$ is estimated from a linear fit to the inner vortex data from April 1 to August 31, 1992. This fit yields a value of 0.43 ±0.05 K/d. The estimation of the sedimentation rate can be made by examining the measurements performed outside the vortex. The region outside the vortex is not sampled during the winter at the altitude of the bulk of the aerosol layer, but some values are detected from the beginning of September. In order to avoid possible bias induced by the particular position of the vortex in October and November, only the measurements obtained far from the vortex edge, e.g., at more than 5° equivalent latitude from the outside vortex border, are selected. The low number of points resulting from this selection does not allow us to provide a correct estimation of the sedimentation in 1992. Furthermore, these values can be affected by two contradicting biases: (1) a decrease of the barycentric potential temperature due to the diabatic descent outside the vortex and also to the mixing at lower levels with air masses originating from the vortex region and (2) an increase linked to the influx of volcanic aerosols from lower latitude regions favorized by the planetary wave activity most intense in the winter stratospheric surf zone [*Trepte et al.*, 1993; *Randell et al.*, 1993]. In consequence, the temporal evolution of Θ_{bar} was extended up to April 1993. Figure 7 shows that the barycentric potential temperature of the aerosol layer in the beginning of 1993, after the interruption of the measurements in the summer period, is comparable to the values observed in the spring of 1992. The comparison of the barycentric potential temperature layer between March 1992 and March 1993 shows that the particles have descended from ~ 480 K down to 430 K isentropic level. A linear fit applied to these data yields a value of 0.13 K/d, which provides a first estimation of $d\theta_s/dt$. Another method for evaluating the influence of the sedimentation consists in computing the sedimentation velocity of the particles. This velocity can be estimated from a linear fit applied to the evolution of the barycentric altitude of the aerosol layer on the same time period of 1 year in order not to be affected by the bias discussed before. The barycentric altitude is defined in the same way as in (1), except that the potential temperature is replaced by the geometrical height. The fit yields a value of 9 m/d. As a comparison, *Chazette et al.* [1995] found 8.3 10^{-3} cm/s or 7.2 m/d with aerosol lidar measurements performed in the northern midlatitude region. Optical counter measurements of the volcanic aerosol size distribution in Antarctica in 1992 show an average radius of 0.3 μm [*WMO*, 1999]. From *Prupacher and Klett* [1980], the fall velocity of a spherical particle of 0.3 μm is about 10^{-2} cm/s or 8.6 m/d around 15 km, so the value of the volcanic aerosol sedimentation velocity outside the vortex compares well with values found in the literature. Taking into account the lowering of the aerosol layer, an average gradient of the potential temperature versus altitude of 15 K/km is found for the measurements obtained inside the vortex from April 1 to August 31 1992. A very small potential temperature tendancy of -0.02 K/d is found during the same period which yields a value of 0.155 K/d for the descent rate due the sedimentation. The diabatic descent rate $d\theta_d/dt$ amounts thus for the measurements performed inside the vortex in the fall and winter period, to 0.25 - 0.3 K/d with an uncertainty evaluated from the precision of the fit and the estimation of the sedimentation rate to about 0.2 K/d at 95% confidence interval. Since the present estimation of the subsidence ignores the influence of quasi-horizontal transport and mixing inside the vortex, the uncertainty of the result might be larger. Radiative transfer calculations performed by *Rosenfield et al.* [1994], in the 1992 winter indicate that at 50 mbar the maximum cooling in the southern hemisphere is toward the pole in April where the highest temperatures are found. However after May, temperatures are lower within the vortex, resulting in the maximum cooling being at the edge and exterior to the vortex. Our results, which cover the lower stratosphere around 400 K, show that the descent of the aerosol layer is strongest inside the vortex. The equivalent latitude range spanned by the measurements during the time period considered here is 8°with an average distance to the inner vortex border of 4°. If this region corresponds to a local maximum of subsidence, neglecting the effect of horizontal mixing which has for effect to weaken the aerosol meridional gradient, leads to an underestimation of the subsidence rate. Besides, it is not possible to evaluate the subsidence outside the vortex with these measurements, since they are affected by the quasi-horizontal transport within the surf zone which leads to an inflow of high aerosol contents from lower latitudes during the winter season.

In *Rosenfield et al.* [1994], air parcels located inside the vortex at about 425 K in April 1992 fell 50 K to 375 K by the end of August. The corresponding subsidence rate of 0.33 K/d compares well with our estimate, although this result corresponds to an average over the whole vortex area. According to the radiative model calculations, the subsidence stops in July at these levels, while our measurements still show a descent in August. In another study dealing with the same 1992 winter, *Manney et al.* [1994] computes higher diabatic descent rates ranging from 0.6 K/d in early winter to 0.4 K/d in the late winter at 420 K in a region close to the vortex edge, using trajectory calculations and vertical velocities from a radiative scheme in order to

study the three-dimensional motion of air in the stratospheric polar vortex. Besides, *Schoeberl et al.* [1992] found subsidence rates close to 0.2 K/d using the ER2 measurements of tracers during the Airborne Antarctic Ozone experiment (AAOE) campaign which took place in August-September 1987. The subsidence rate evaluated in the present study compare rather well with these estimations, despite their relative dispersion linked to the differences in the season or the area considered. This result, together with the study on the permeability of the polar vortex, supports the idea of "containment vessel" for the polar vortex [*McIntyre,* 1995] and is in contradiction with the estimated value of 1.3 K/d in the lower stratosphere by *Tuck et al.* [1993] which lead to the hypothesis of "flowing processor."

5.2. Ozone Measurements

The air subsidence can also be estimated from the evolution of the ozone mixing ratio as a function of time in autumn, in the region of maximum ozone mixing ratio vertical gradient, that is up to ~ 500 K. The method is detailed by *Bergeret et al.* [1998]: the average descent rate $d\theta/dt$ is derived from the difference in potential temperature between the average ozone profile prior to the vortex formation and the average ozone profile computed from the measurements performed inside the vortex in July before the beginning of the ozone destruction, assuming that the ozone mixing ratio is conserved during the diabatic descent. The ozone profiles are averaged as a function of potential temperature in order to reduce the variability linked to adiabatic processes. Small-scale local processes are smoothed out by the averaging but the mean ozone profiles are further smoothed using a five points running mean in order to suppress the residual small-scale variability and focus on the subsidence only. An alternative method for estimating the subsidence rate uses the temporal evolution of the ozone mixing ratio combined with the average ozone gradient as a function of the potential temperature in the considered time period. Considering the sampling of the ozone field by the Dumont d'Urville data, the first method allows us to obtain results less sensitive to the day-to-day variability of the ozone mixing ratio isentropic gradient. Figure 8 shows the subsidence rates obtained with the ozone data in the years 1994 and 1996 together with the rate deduced from the volcanic aerosol data in 1992. The error bars correspond to 95% confidence interval. The results from the ozone data show an increase of the subsidence as a function of the potential temperature, which was expected since radiative model calculation show a stronger descent in the middle and upper stratosphere. Besides, they are in good agreement with the estimates of trace gas descent in the Antarctic vortex using HALOE data, by *Schoeberl et al.* [1995]. The error bars of the estimated subsidence rates are relatively large. Moreover, our estimation, as indicated previously, depends on the data sampling in Dumont d'Urville and is not free from possible artefacts linked to mixing processes within the vortex during the time period considered, so the interannual variability shown by these results should be considered with caution.

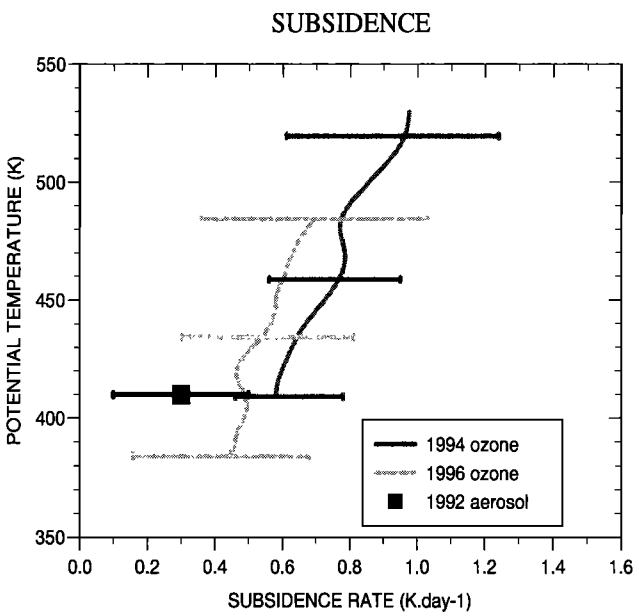

Figure 8. Evaluation of the subsidence rates in autumn from ozone measurements in 1994 and 1996 and from aerosol measurements in 1992. The error bars correspond to 95% confidence interval.

6. Analysis of the Ozone Destruction

The ozone destruction rate due to heterogeneous chemistry can be computed from the temporal evolution of the ozone mixing ratio displayed in Figure 5. The analysis of the ozone seasonal variation in the various regions showed that the ozone destruction takes place mostly inside the vortex or in the inner vortex edge from 400 to 550 K. Some particular measurements can, however, be noticed during the destruction period, like those showing high ozone values inside the vortex in 1993, in the beginning of September and in mid-October: In the first case, two measurements were obtained, by lidar and by sonde. Both show an increase of ozone between 400 and 500 K, while the analysis of the potential vorticity field gives an equivalent latitude of Dumont d'Urville of 70.6°S, at about 8° of the inner vortex border. In October the higher ozone value is provided by a sonde measurement showing a peak of ozone from 450 to 500 K, while the station is at 1.5° of the inner vortex border. Similarly, some measurements classified as outside the vortex show rather low ozone amounts in September 1996. These outliers indicate either an error in the position of the station with respect to the polar vortex or local dynamical events which are not detected by the PV analysis. Complete understanding of these measurements would require the use of a high-resolution transport model in order to determine more precisely

the location of the vortex edge at the time of the measurement. In contrast, the low ozone values detected outside the vortex in October 1997 correspond to near tropical air, as mentioned in section 4. Owing to the poorer sampling of the edge region in winter and the higher variability on the ozone amounts, only the measurements performed inside the vortex are considered for the derivation of the destruction rates. The exact starting date of the ozone depletion at the various levels is difficult to determine precisely, owing to the alternate sampling of the inner vortex and edge regions in winter and the inherent ozone variability in each region. The first signs of decrease are generally detected in the first 2 weeks of August at the various levels. At 400 K, only the inner vortex and edge regions are sampled in winter so the distinction between the regions where the destruction takes place and the outside region can be made only to some extent from the end of August. The ozone destruction lasts generally up to the end of September at the various levels. The ozone amounts remain low inside the vortex and in the inner edge up to the end of October and beginning of November which corresponds to the end of the measurement period in the case of the lidar measurements.

The ozone loss rates are computed from linear fits to the inner vortex data at the various isentropic levels, during the ozone destruction period. These rates are indicated in % per day in Table 2 with the time period of the calculation. The percentages are computed with respect to the average mixing ratio within the time period of the fit. The time period can be different for the various levels in one particular year since it depends on the minimum altitude of a lidar measurement or the maximum altitude reached by an ozone sounding. The results presented here expand the results of *Bergeret et al.* [1998] who analyzed the ozone destruction from 1993 to 1996. The ozone loss rates estimated here are lower limits for the chemical destruction since the diabatic descent can partially compensate the ozone decrease in the lower stratosphere. The heating rate computed by *Rosenfield et al.* [1994] in the 1987 and 1992 austral winter were used to estimate the effect of the subsidence in spring. According to this study, the heating rates averaged in the Southern Hemisphere vortex are of the order of -0.1 K/d in the August-September period, which converts roughly to 0.2 K/d in diabatic descent rate. Considering an average ozone gradient of 6 ppbv/K and an average ozone mixing ratio of 1 ppmv in the 350-500 K potential temperature range, estimated from the measurements performed inside the vortex during this period, the effect of the subsidence amounts to $\sim$ 1.2 ppbv/d or 0.12 %/d. The low value of the ozone average gradient is itself due to the ozone destruction. The effect of eddy horizontal mixing was estimated by *Schoeberl et al.* [1992] for the AAOE campaign. They found an ozone tendency linked to this process, of 6.2×10^{-2} %/d around 70°S at 420 K. Consequently, the contributions of the subsidence and horizontal mixing can be neglected at a first order, taking into account the error bars on the estimates. Finally, in order to compare with other Antarctic ozone loss rates reported in the literature, Table 3 shows the ozone loss rates derived in Dumont d'Urville at 475 K in ppbv/d and at 18 km in DU/d. Table 3 indicates also the number of points used in the linear fit at 475 K, the quality of the fit represented by the square of the correlation coefficient r^2, and the equivalent latitude range covered by the measurements compared with the average position of the border in equivalent latitude.

The maximum ozone loss rates are computed in 1993, a year when the inner vortex region was correctly sampled by the ground-based measurements. At 475 K, the destruction rate estimated from the Dumont d'Urville data which correspond to 65 ppbv/d as shown in Table

Table 2. Ozone Loss Rates From the Measurements Performed Inside the Vortex

Level	Year	1993	1994	1996	1997	1998
400 K	Period	236-284	218-295	222-274	223-280	221-260
	Rate	3.6	> 1.8	2.5	3.4	3.0
	Uncertainty	0.8	0.6	0.8	1.1	0.8
430 K	Period	236-259	213-298	222-274	237-280	221-260
	Rate	3.9	> 1.4	$\geq$ 2.7	3.4	2.7
	Uncertainty	4.0	0.4	0.8	0.9	1.0
475 K	Period	236-269	213-298	222-274	237-268	221-260
	Rate	4.3	> 1.1	$\geq$ 2.2	2.0	2.7
	Uncertainty	2.2	0.5	0.4	4.0	1.0
550 K	Period	236-273	226-296	222-274	217-268	221-260
	Rate	1.9	> 0.7	$\geq$ 0.5	0.8	1.3
	Uncertainty	0.6	0.4	0.6	1.6	0.5

The ozone loss rates and the error estimation are in % per day. The error corresponds to 95% confidence interval. The time period of the estimation is expressed in Julian day.

Table 3. Ozone Loss Rates at 475 K in ppbv/d Together With Two Sigma Uncertainty, the Number of Points of the Fit, the Quality of the Fit Represented by r^2 , the Equivalent Latitude Range Covered by the Measurements, the Average Equivalent Latitude of the Inner Vortex Border, and the Ozone Loss Rate at 18 ± 1 km in DU/d

	1993	1994	1996	1997	1998
Loss rate at 475 K	65 ± 35	> 30 ± 14	≥ 30 ± 6	32 ± 64	48 ± 19
Number of points	8	8	13	5	11
r^2	0.70	0.76	0.90	0.25	0.73
Equivalent latitude range	67.5°S ± 2.7	67.9°S ± 4.6	67.6°S ± 3.7	69.4°S ± 3.6	65.5°S ± 3.6
Inner vortex border	62.8°S	62.9°S	63.1°S	64.2°S	61.2°S
Loss rate at 18 km	0.97 ± 0.5	> 0.48 ± 0.18	≥ 0.46 ± 0.12	0.42 ± 0.34	0.9 ± 0.22

3, compares well with the values derived from the McMurdo ozone soundings for September 1993 [*Johnson et al.*, 1993]. They are 30% lower than the loss rate evaluated from ozone soundings at the South Pole station by *Hofmann et al.* [1997], which was the highest in a 10-year period ranging from 1986 to 1995. In 1994, the measurements performed inside the vortex in August do not show any decrease except at 400 K. There was no sampling of the inner vortex region in September so the destruction rates at various levels are computed by using the August measurements inside the vortex and a single measurement performed in the second half of October. The values given in Table 2 provide thus at best a minimum estimate of the destruction rate since the end of the destruction period occurs generally around the end of September. The rate estimated in Dumont d'Urville corresponds to less than half of the rate computed at South Pole for the same year. The best sampling of the ozone field was obtained in 1996 with 91 ozone measurements in total and 41 concentrated in the August-October period. However, if the inner vortex region is well sampled in August, it is not the case in September when all the measurements are performed at the edge or outside the vortex. The destruction rates shown in Table 2 are computed from mid-August to the end of September when the measurements sample again the vortex. Most of the measurements used in the fit were made in August and only two at the end of September. At this time, the measurements show near zero ozone values up to 475 K. So the destruction rates could represent a lower estimate, had the ozone destruction been faster in September. The destruction rates computed with the August measurements only amount to 2.8, 3.0, and 2.8%/d at 400, 430, and 475 K, respectively. They are 3 times larger than the rates deduced from the POAM II data [*Bevilacqua et al.*, 1997] during the same period. This difference may originate from a different sampling of the ozone field, since that during this period, the satellite was deeply inside the vortex, from 72° to 83° latitude south, whereas Dumont d'Urville remains mainly at 4°equivalent latitude in average of the inner vortex boundary. This is consistent with an ozone depletion starting earlier near the border of the vortex than in the center [*Roscoe et al.*, 1997]. At 550 K the ozone amount is rather low in August as compared to other years and comparable to the values found at the end of September. The data present a large variability, which is reflected in the large error bar of the destruction rate. In 1997, the inner vortex region was poorly sampled, and the linear fits rely on five measurements only performed in this region from mid-August to the end of September. The ozone values are particularly noisy at 475 and 550 K, which prevents to deduce reliable destruction rates at these levels, as indicated by the value of r^2. In 1998, a good sampling of the vortex was achieved up to mid-September, and the destruction rates of about 3 %/d are reliable for this period.

In order to check the reliability of the results obtained here, a sensitivity study was conducted on the ozone losses obtained at 475 K, with a selection of the inner vortex data at more than 2° equivalent latitude (in absolute value) from the inner vortex border. The number of points of the linear fit is then reduced to 7, 5, 10, 4, and 8 from 1993 to 1998, respectively, and the r^2 values are slightly increased. The new ozone loss rates are very similar to the ones indicated in Table 3 except for the year 1997, which shows a doubling of the initial value. This test confirms that the ozone losses derived in Dumont d'Urville are reliable when the inner vortex is correctly sampled by the measurements.

As a conclusion, the analysis of lidar and sondes measurements in Dumont d'Urville yields ozone loss rates on the order of 3 %/d or more depending on the year, in the 400-475 K region. The destruction generally takes place from the first half of August and is nearly complete by the end of September in the 400-475 K range. A lower rate of about 1.5 %/d is obtained at 550 K. The destruction is not complete at this level, and the lowest ozone amounts reach ~ 1 ppmv. These results characterize the ozone destruction in a region located between 65 and 70°S equivalent latitude sampled in average by the ground-based measurements performed inside the vortex during the August-September period.

7. Analysis of the Vortex Containment in Spring as a Function of Potential Temperature

It is possible to study the vortex containment from the ozone measurements when the ozone mixing ratio is stable as a function of time. A good period is October, when the ozone amounts are still low and relatively stable in the polar vortex after the ozone destruction (see Figure 5). Since the data sampling in the various regions must be statistically sufficient, we focus on October 1996 when 14 ozone lidar and 3 ECC sondes measurements were performed. Figure 9 represents the ozone mixing ratio as a function of the difference between the equivalent latitudes of Dumont d'Urville and the vortex limit in October 1996, with the same symbols as in Figure 5. Despite the less stability of ozone values in September owing to the still occuring ozone destruction, September data are added to Figure 9 in order to provide a better view of the outside region which was well sampled during this month. Figure 9 shows that the ozone difference between the inside and the outside vortex regions increases substantially from 400 to 650 K (note the different ozone range at 650 K). This indicates a higher exchange of air between both regions in the lower than in the middle stratosphere, in agreement with previous studies such as *Tuck et al.* [1989], *Manney et al.* [1994] and *Wauben et al.* [1997]. The very low ozone values observed inside the vortex at 475 K together with the steepness of the ozone gradient accross the vortex edge are a further evidence of the vortex isolation at this isentropic level. At 400 K, the ozone values in September are higher in the edge region than outside the vortex. This feature is also observed to a lower extent at 475 K. These high ozone values can be due to a maximum in diabatic descent near the vortex edge, as calculated by *Manney et al.* [1994] and *Schoeberl et al.* [1992].

At 475 and 550 K, the ozone amounts in the edge region show rather well the transition between the inside

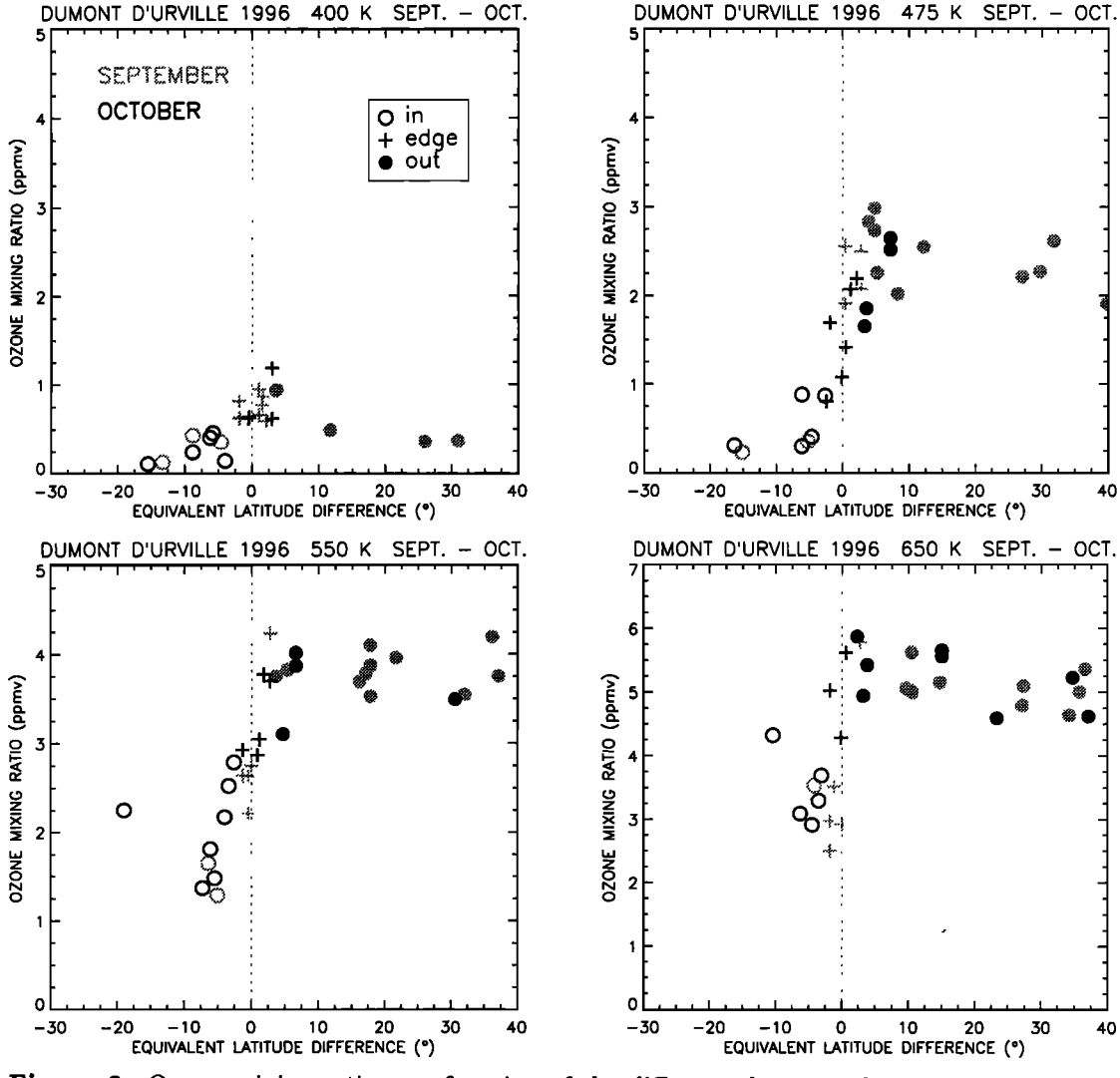

Figure 9. Ozone mixing ratio as a function of the difference between the equivalent latitudes of Dumont d'Urville and the vortex limit, in September and October 1996, at various isentropic levels. The symbols are similar to those used in figure 5.

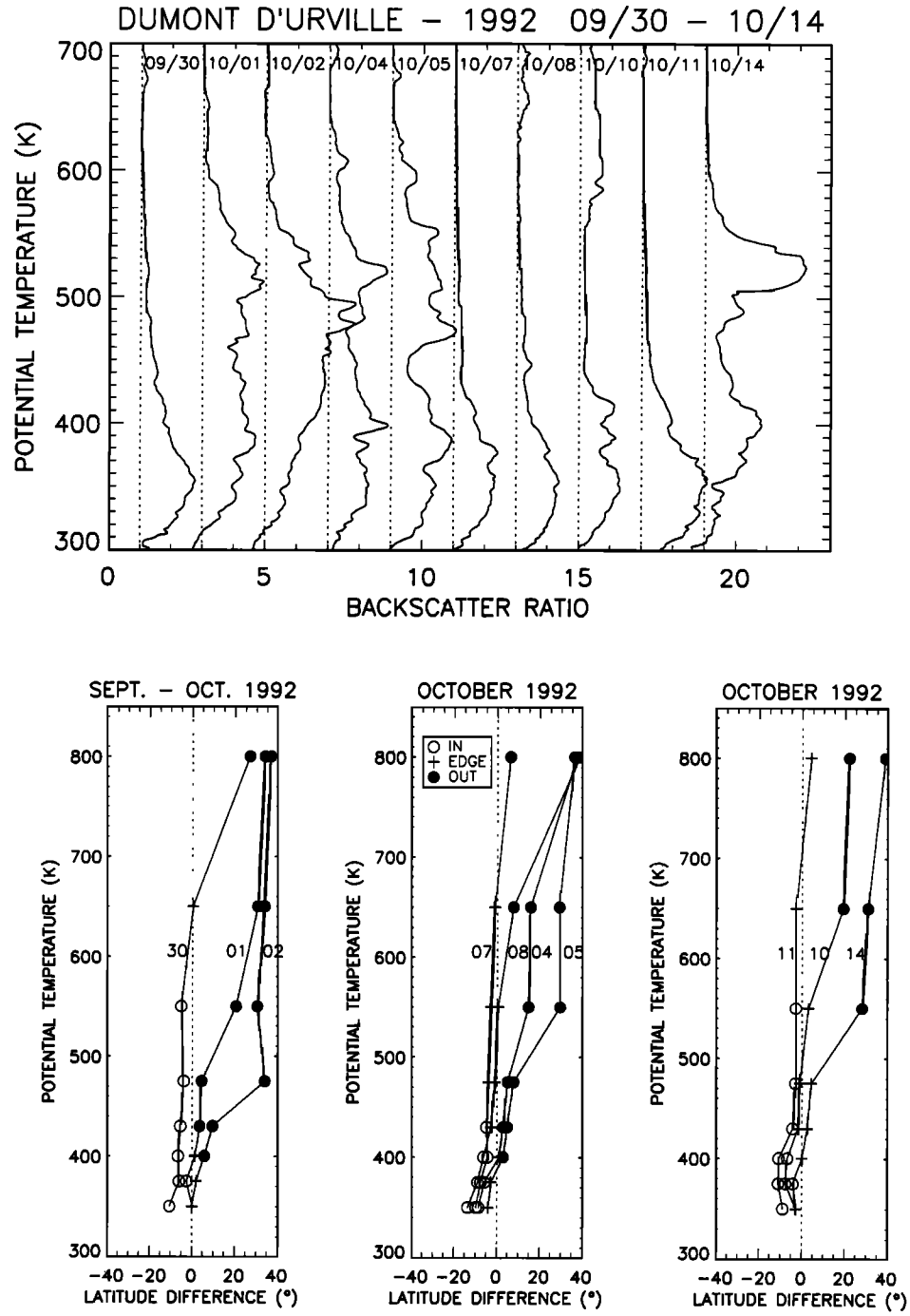

Figure 10. (top) Temporal evolution of the aerosol backscatter ratio profiles from September 30 to October 14, 1992. (bottom) Difference between the equivalent latitude of Dumont d'Urville and the vortex limit as a function of potential temperature for the days when aerosols lidar measurements were obtained. The date of each profile is indicated.

and the outside regions, the inner edge region data being affected by the destruction while the outer edge data are close to the outside vortex values. This confirms the notion of vortex limit defined by the maximum PV gradient in the edge region. At 475 K, however, some low ozone amounts classified as "outside the vortex" are noticeable in September and October, close to the vortex edge. These data could indicate a local transport of ozone depleted air masses to the outside region or an error in the classification. Likewise, high ozone amounts classified as "inside the vortex" are found at 550 K. This underlines the difficulty to define precisely the inner and outer borders of the vortex from the PV fields. At 650 K, the data show an ozone decrease as a function of equivalent latitude with a high difference between the inside and the outside vortex regions. This difference is due to the the natural meridional ozone gradient in the middle stratosphere.

A finer view of the vortex edge can be gained from the aerosol lidar measurements performed in October and November 1992. During this period, a long series of aerosol lidar measurements was performed while the vortex was deformed by planetary waves and elongated, in the middle stratosphere. In consequence, most of the measurements were made inside the vortex in the low stratosphere and alternatively inside and outside the vortex in the middle stratosphere as the deformed vortex passed above the station. Part of these measurements are presented in Figure 10 (top) which shows the aerosol lidar backscatter ratio shifted by 2 for each day from September 9 to October 14. Figure 10 (bottom) shows the position of the station expressed in distance to the vortex limit in equivalent latitude. The date of the measurement is indicated on each curve. During this period, some measurements are performed entirely inside or at the edge of the polar vortex (September 30, October 7 and 11), while others are made inside or in the edge region in the lower levels and outside above. In 1992, the vortex did not break before mid-November or later in the altitude range studied here. Figure 10 shows that when the aerosol measurements sample the outside region in the upper levels, rather high aerosol amounts are detected, whereas low amounts are measured a few days later when the measurements sample the inner vortex or the edge region. The measurements performed entirely inside the vortex show a single aerosol layer peaking at 350 K. Those performed entirely outside (October 2 for instance) show also a single aerosol layer peaking slightly under 500 K. The measurements performed inside the vortex or in the vortex edge in the lower stratosphere and outside the vortex above (October 5 or 14) present two aerosol layers. The transition between the layers can be quite sharp as on October 14, which shows a strong aerosol gradient above 500 K as the laser beam leaves the vortex edge region and penetrates the surf zone. These measurements clearly visualize the stratified structure of the vortex edge and demonstrate the low degree of mixing prevailing in this region above 400 K. Furthermore, ozone sounding measurements performed during the same period show also the features characteristics of each region crossed by the sonde during the balloon ascent (very low ozone values in the lower stratosphere, high ozone amounts characteristics of the outside region in the middle stratosphere). These results support the already mentioned studies on the permeability of the vortex edge, using a contour advection technique and a semi lagrangian transport model [*Chen*, 1994; *Chen et al.*, 1994]. These studies, which investigate the lengthning of PV contours, suggest the existence of a transition layer around the 400 K isentropic surface, above which the vortex is near completly isolated from the midlatitudes and below which the vortex is less isolated.

8. Conclusion

The ground-based measurements of the ozone and aerosol vertical profile performed in the Dumont d'Urville station located at the shore of the Antarctic continent allow a detailed study of the region surrounding the vortex edge on an interannual basis. The variability of the aerosol and ozone amounts linked to the position of the station with respect to the polar vortex requires the development of classifying tools using the concept of equivalent latitude. After classification, the examination of the measurements temporal evolution allows us to identify the main processes affecting the air inside the vortex and in the vortex edge such as the subsidence and the springtime ozone depletion. If the subsidence is observed on all the measurements indifferently of the region sampled, the ozone destruction processes affect mainly the inner vortex and inner edge regions. The subsidence rate of about 0.3 K/d around 400 K estimated in this work is in good agreement with radiative model estimates, considering the differences in areas and time periods in the various studies. The subsidence rates deduced from the ozone measurements under 500 K compare well with estimates from trace gas descent using satellite data. They support the idea of relative vortex isolation above 400 K [*WMO*, 1999]. Our results show that the ozone destruction affects mainly the region located between 400 K (the lower level considered in this study) and 550 K, from early August to the end of September. At this time period, near zero ozone amounts are found up to 475 K. No clear ozone destruction is observed at 650 K, but it might be compensated by dynamical effects. The destruction rates derived from the measurements are strongest around 475 K where they can exceed 3 - 4%/d, depending on the year. For each year, the precision of our estimate depends on the sampling by the measurements of the regions affected by the depletion processes. If this sampling is generally good in August when the vortex reaches its largest size and is the most stable, it is less the case in September when planetary waves can distort the vortex, as shown by the higher variablity of Dumont d'Urville equivalent latitude in the springtime. The very low ozone amounts observed systematically inside the vortex in October at 475 K demonstrate the isolation of the vortex at this altitude range. Besides, a measurements series of the aerosol vertical profile in October 1992, a period when the vortex was distorted by planetary waves, shows the details of the edge region and the sharp tracer gradient between the various regions.

Owing to the strong atmospheric gradients linked to the proximity of the polar vortex edge, the comparison of the Dumont d'Urville data with satellite measurements in the fall to spring period is likely to be improved by the projection of the data in the potential temper-

ature - equivalent latitude framework. Furthermore, in this coordinate system the good sampling of the ozone field by some of the satellite measurements available in the polar regions should allow the estimation of ozone destruction rates as a function of equivalent latitude and not averaged on an area sampled by ground based measurements. Such a study was conducted recently by *Bergeret* [1999] using Microwave Limb Sounder (MLS) data averaged in equivalent latitude bins. The comparison of the destruction rates with the results obtained in the present work shows a good agreement in 1993. Higher destruction rates are deduced from the satellite data from the end of August to mid-September in 1994 and 1996, in the 65°to 70°S equivalent latitude region, which confirms the hypothesis of underestimation of the ozone destruction from the ground-based measurements, in the case of an insufficient sampling of the inner vortex region in September.

Finally, the measurements performed in Dumont d'Urville show cases of ozone or aerosol amounts which do not fit in the regions where they are classified. Such measurements could indicate transport of air from inside the vortex to the outside region or conversely. The analysis of such events requires the use of high-resolution transport models in order to define more precisely the edge of the vortex. One of these models is presently used for the study of filamentation events in the Northern Hemisphere [*Hauchecorne et al.*, 1998; *Marchand et al.*, 1999] and will be run in the next future in the Antarctic to understand these particular measurements.

Acknowledgments. The authors are grateful to the Institut Français de la Recherche et de la Technologie Polaire (IFRTP) for providing support to the Stratospheric Ozone project in Antarctica and for the operation of the lidar at Dumont d'Urville. In particular, they wish to thank the various "Geophy" teams who provided each year very valuable data in a remote environment. They also want to thank Anne Garnier for the technical coordination of the lidar measurements as well as Jacques Porteneuve and Frédéric Fassina for their technical support. The present work was funded by the European project SAONAS (Stratospheric Aerosol and Ozone in the Northern and Southern hemisphere, ENV4-CT95-0090) and by the French "Programme National de Chimie Atmospherique" of the Centre National de la Recherche Scientifique (CNRS).

References

Bergeret, V., S. Bekki, S. Godin, and G. Mégie, Analyse des variations saisonnières de l'ozone antarctique dans la basse stratosphère à partir des données lidar et sonde de Dumont d'Urville, *C. R. Acad. Sci., Ser. II, 326,* 751-756, 1998.

Bergeret, V., Analyse de l'ozone dans la basse stratosphère de l'Hémisphère Sud à l'aide du concept de latitude équivalente, PhD thesis, 219 pp., Paris VI Univ., Paris, 1999.

Bevilacqua, R. M., et al., POAM II ozone observation in the Antarctic ozone hole in 1994, 1995 and 1996, *J. Geophys. Res., 102,* 23,643-23,657, 1997.

Bowman, K. P., Large-scale isentropic mixing properties of the Antarctoc polar vortex from analyzed winds, *J. Geophys. Res., 98,* 23,013-23,027, 1993.

Butchart, N., and J. Austin, On the relationship between the quasi-biennal oscillation, total chlorine and the severity of the antarctic ozone hole, *Q. J. R. Meteorol. Soc., 122,* 183-217, 1996.

Butchart, N., and E. Remsberg, The area of the polar vortex as a diagnostic for tracer transport on an isentropic surface, *J. Atmos. Terr. Phys., 43,* 1319-1339, 1986.

Chazette, P., C. David, J. Lefrère, S. Godin, J. Pelon, and G. Mégie, comparative study of the optical, geometrical, and dynamical properties of post-volcanic aerosols, following the eruptions of El Chichon and Mount Pinatubo, *J. Geophys. Res., 100,* 23,195-23,207, 1995.

Chen, P., J. R. Holton, A. O'Neill, and R. Swinbank, Quasi-horizontal transport and mixing in the Antarctic stratosphere, *J. Geophys. Res., 99,* 16,851-16,866, 1994.

Chen, P., The permeability of the Antarctic vortex edge, *J. Geophys. Res., 99,* 20,563-20,571, 1994.

Chipperfield, M. P., M. L. Santee, L. Froidevaux, G. L. Manney, W. G. Read, J. W. Waters, A. E. Roche, and J. M. Russel, Analysis of UARS data in the southern polar vortex in September 1992 using a chemical transport model, *J. Geophys. Res., 101,* 18,861-18,881, 1996.

David, C., S. Bekki, S. Godin, G. Mégie, and M. P. Chipperfield, Polar Stratospheric Clouds climatology over Dumont d'Urville between 1989 and 1993 and the influence of volcanic aerosols on their formation, *J. Geophys. Res., 103,* 22,163-22,180, 1998.

Deniel, C., R. M. Bevilacqua, J. P. Pommereau, and F. Lefèvre, Arctic chemical ozone depletion during the 1994-1995 winter deduced from POAM II satellite observations and the REPROBUS three-dimensional model, *J. Geophys. Res., 103,* 19,231-19,244, 1998.

Deshler, T., B. J. Johnson, and W. R. Rozier, Balloonborne measurements of Pinatubo aerosols during 1992 at 41°N: vertical profiles, size distribution and volatility, *Geophys. Res. Lett., 20,* 1435-1438, 1993.

Godin, S., C. David, L. Stefanutti, M. Del Guasta, and M. Morandi : Ozone and aerosols lidars measurements in 1991 and 1992 in Dumont d'Urville, *in Conference Proceedings "Italian Research on Antarctic Atmosphere",* edited by Colacino et al., 283-294, Soc. Italiana di Fisica, Porano, Italy, 1992.

Godin, S., et al., Systematic stratospheric observations on the Antarctic continent at Dumont d'Urville, *in Proceedings Quad. Ozone Symp., 561, NASA Conf. Publ. 3266,* 561-564, 1994a.

Godin, S., G.Mégie, C.David, V. Mitev, D. Haner, Y. Emery, C. Flesia, V. Rizi, G. Visconti, and L. Stefanutti, Ozone, aerosols and polar stratospheric clouds measurements during the EASOE campaign, *Proceedings Quad. Ozone Symp., 561, NASA Conf. Publ. 3266,* 550-553, 1994b.

Godin, S., C. David, and M. Guirlet, Evolution of the Mt. Pinatubo volcanic cloud and analysis of its effect on the ozone amount as observed from ground-based measurements performed in northern and southern latitudes, *NATO ASI Ser. I 42,* 143-159, 1996.

Hamill,P., H. Houben, R. Young, R. Turco, and J. Zhao, Microphysical Processes affecting the Pinatubo volcanic plume, *NATO ASI Ser. I 42,* 49-59, 1996.

Hauchecorne, A., S. Godin, and C. Souprayen, Meridional transport of ozone in the lower stratosphere at middle latitudes: lidar observation and simulation with a high resolution advection model, paper presented at 23rd Gen-

eral Assembly, Eur. Geophy. Soc., Nice, France, April 1998.

Hofmann, D. J., S. J. Oltmans, J. M. Harris, B. J. Johnson, and J. A. Lathrop, Ten years of ozonesonde measurements at the south pole: Implication for recovery of springtime Antarctic ozone, *J. Geophys. Res., 102,* 8931-8943, 1997.

Johnson, B. J., T. Deshler, and R. Zhao, Ozone profiles at McMurdo station, Antarctica during the spring of 1993: Record low ozone, *Geophys. Res. Lett., 22,* 183-186, 1995.

London, J., The observed distribution and variations of total ozone, in *Ozone in the Free Atmosphere,* edited by R. C. Whitten and S. S. Prasad, pp. 11-80, Van Nostrand Reinhold Co., New York, 1985.

Manney, G. L., and W. Z. Zureck, Interhemispheric comparison of the development of the stratospheric polar vortex during fall: A 3-Dimensional perspective for 1991-1992, *Geophys. Res. Lett., 20,* 1275-1278, 1993.

Manney, G. L., R. W. Zurek, A. O'Neill, and J. W. Waters, On the motion of air through the stratospheric polar vortex, *J. Atmos. Terr. Phys., 51,* 2973-2994, 1994.

Manney, G. L., R. W. Zurek, L. Froidevaux, J. W. Waters, A. O'Neill, and R. Swinbank, Lagrangian transport calculations using UARS Data, Part II: Ozone, *J. Atmos. Sci., 52,* 3069-3081, 1995.

Marchand, M., S. Godin, and A. Hauchecorne, Study of the Antarctic Polar Vortex erosion from ozone lidar measurements performed at OHP (44°N, 6°E), paper presented at 24th General Assembly, Eur. Geophy. Soc., La Haye, Netherlands, 1999.

McIntyre, M. E., The stratospheric polar vortex and subvortex: Fluid dynamics and midlatitude ozone loss, *Philos. Trans. R. Soc. London, Ser. A, 352,* 227-240, 1995.

McIntyre, M. E., and T. Palmer, The "surf zone" in the stratosphere, *J. Atmos. Terr. Phys., 46,* 825-849, 1984.

McPeters, R. D., The atmospheric SO_2 budget derived for Pinatubo from NOAA-11 SBUV/2 spectral data, *Geophys. Res. Lett., 20,* 1971-1974, 1993.

Nash, E. R., P. A.Newman, J. E. Rosenfield, and M. E. Schoeberl, An objective determination of the polar vortex using Ertel's potential vorticity, *J. Geophys. Res., 101,* 9471-9478, 1996.

Pommereau, J. P., and F. Goutail, Stratospheric O3 and NO2 Observations at the Southern Polar Circle in Summer and Fall 1988, *Geophys. Res. Lett., 15,* 895-898, 1988.

Pruppacher H. R., and J. D. Klett, *Microphysics of Clouds and precipitation,* 714 pp., D. Reidel, Norwell, Mass., 1980.

Randel, W. J., J. C. Gille, A. E. Roche, J. B. Kumer, J. L. Mergenthaler, J. W. Waters, E. F. Fishbein, and W. A. Lahoz, Stratospheric transport from the tropics to middle latitudes by planteray-wave mixing, *Nature, 365,* 533-535, 1993.

Rex, M, et al., Prolonged stratospheric ozone loss in the 1995-1996 winter, *Nature, 389,* 835-838, 1997.

Ricaud, P., et al., The stratosphere over Dumont d'Urville, Antarctica, in winter 1992, *J. Geophys. Res., 103,* 13,267-13,284, 1998.

Roscoe, H. K., A. E. Jones, and A. M. Lee, Midwinter start to Antarctic azone depletion: Evidence from observations and models, *Science, 278,* 93-96, 1997.

Rosenfield, J. E., P. A. Newman, and M. R. Schoeberl, Computation of diabatic descent in the stratospheric polar vortex, *J. Geophys. Res., 99,* 677-689, 1994.

Schoeberl, M. R., L. R. Lait, P. A. Newman, and J. E. Rosenfield, The Structure of the polar vortex, *J. Geophys. Res., 92,* 7859-7882, 1992.

Schoeberl, M. R., M. Luo, and J. E. Rosenfield, An analysis of the Antarctic Halogen Occultation Experiment trace gas observations, *J. Geophys. Res., 100,* 5159-5172, 1995.

Schulz, A., et al., Match observations in the Arctic winter 1996/97: High stratospheric ozone loss rates correlate with low temperatures deep inside the polar vortex, *Geophys. Res. Lett., 27,* 205-208, 2000.

Solomon, S., Stratospheric Ozone depletion: A review of concepts and history, *Rev. Geophys., 37,* 275-316, 1999.

Stefanutti, L., M. Morandi, M. Del Guasta, S. Godin, G. Mégie, J. Brechet, and J. Piquard, Polar stratospheric cloud observations over the Antarctic continent at Dumont d'Urville, *J. Geophys. Res., 96,* 12,975-12,987, 1991.

Stefanutti, L., F. Castagnolli, M. Del Guasta, M. Morandi, V.M. Sacco, L. Zuccagnolli, S. Godin, G. Mégie, and J. Porteneuve, The Antarctic ozone lidar system, *Appl. Phys. B, 55,* 3-12, 1992

Trepte, C. R., R. E. Veiga, and M. P. McCormick, Poleward dispersal of Mount Pinatubo volcanic aerosol, *J. Geophys. Res., 98,* 18,562-18,573, 1993.

Tuck, A. F., Synoptic and chemical evolution of the Antarctic vortex in late winter and early spring, 1987, *J. Geophys. Res., 94,* 11,687-11,737,1989.

Tuck, A. F., J. M. Russell III, and J. E. Harries, Stratospheric dryness: Antiphased dessication over Micronesia and Antarctica, *Geophys. Res. Lett., 20,* 1227-1230, 1993.

Uchino, O., R. D. Bojkov, D. S. Balis, K. Akagi, M. Hayashi, and R. Kajihira, Essential characteristics of the Antarctic-spring ozone decline: Update to 1998, *Geophys. Res. Lett., 26,* 1377-1380, 1999.

Wauben, W. M. F., R. Bintanja, P. F. J. van Velthoven, and H. Kelder, On the magnitude of transport out of the Antarctic polar vortex, *J. Geophys. Res., 102,* 1229-1228, 1997.

World Meteorological Organization, Ozone Assessment 1998, WMO, Rep. 44, Geneva, 1999.

S. Bekki, V. Bergeret, C. David, S. Godin, and G. Mégie, Service d'Aéronomie du CNRS, Université Pierre et Marie Curie, Boite 102, 4 Place Jussieu, 75252 Paris, Cedex 05, France. (sophie.godin@aero.jussieu.fr)

(Received March 13, 2000; revised July 18, 2000; accepted July 25, 2000.)